Polyphase glacial dynamics and clast dispersal patterns in glaciofluvial and glacial sediments in north-central Quebec, with application to diamond exploration

M. Parent[1*]

Parent, M., 2023. Polyphase glacial dynamics and clast dispersal patterns in glaciofluvial and glacial sediments in north-central Quebec, with application to diamond exploration; in *Surficial geology of northern Canada: a summary of Geo-mapping for Energy and Minerals program contributions, (ed.) I. McMartin; Geological Survey of Canada, Bulletin 611, p. 201–219. https://doi.org/10.4095/331425*

Abstract: The regional dynamics of shifting ice-flow directions and ice-divide migrations were es-tab-lished in the Saindon-Cambrien corridor of north-central Quebec by two independent means: 1) the measurement of crosscutting striations; and 2) the glacial dispersal patterns of distinctive lithological markers from outliers of the Sakami Formation. Clasts from two outliers were successively dispersed to the north-northeast, northwest, and west-southwest. They form composite dispersal trains consisting of 200 km long ribbon-shaped trains toward the west-southwest and palimpsest trains caused by the westward re-entrainment of dispersal trains formed during earlier flow phases. Widespread evidence of basal sliding and abrasion recorded by striations associated with successive flow systems, together with the development of long dispersal trains, indicates that protracted warm-based conditions prevailed in north-central Quebec. This improved understanding of glacial dynamics and dispersal in the core region of the eastern Laurentide Ice Sheet helps us to interpret the distribution of legacy kimberlite indicator mineral data sets in eskers and to assess the diamond prospectivity of the Saindon-Cambrien corridor.

Résumé : La dynamique régionale des changements de direction de l'écoulement glaciaire et des migrations des lignes de partage glaciaire dans le corridor Saindon-Cambrien, dans le centre nord du Québec, a été établie au moyen des deux critères indépendants suivants : 1) un levé des stries glaciaires présentant des relations de recoupement; et 2) les configurations régionales de dispersion glaciaire de marqueurs de lithologies distinctives dérivés de lambeaux de la Formation de Sakami. Les clastes provenant de deux de ces lambeaux ont été dispersés successivement vers le nord–nord-est, le nord-ouest et l'ouest–sud-ouest. Ils forment des traînées de dispersion composites, constituées de traînées de dispersion rubanées longues de 200 km vers l'ouest–sud-ouest et de traînées palimpsestes résultant du réentraînement vers l'ouest de traînées de dispersion formées lors de phases d'écoulement antérieures. La présence répandue d'indicateurs de glissement sous-glaciaire et d'abrasion glaciaire, tels les stries formées lors des mouvements glaciaires successifs, ainsi que la formation de longues traînées de dispersion indiquent que des conditions de glace basale tempérée ont longuement prévalu dans le centre nord du Québec. La connaissance accrue de la dynamique et de la dispersion glaciaires dans la région située au cœur du secteur oriental de l'Inlandsis laurentidien nous permet d'interpréter la distribution des minéraux indicateurs de kimberlite dans les eskers et d'évaluer la prospectivité du corridor Saindon-Cambrien pour le diamant

[1]Geological Survey of Canada, 490, rue de la Couronne, Québec, Quebec G1K 9A9
*Corresponding author: M. Parent (email: michel.parent@nrcan-rncan.gc.ca)

INTRODUCTION

The Archean craton of northern Quebec is a vast region with established diamond potential (Moorhead et al., 2000). Nevertheless, except for a few large-scale surveys by private firms (Ashton-Soquem, BHP, De Beers), the region is underexplored relative to other comparable areas in Canada. For this reason, Natural Resources Canada, through programs such as the Northern Resources Development program and the Targeted Geoscience Initiative, funded a joint Geological Survey of Canada–Ministère des Ressources naturelles project to remedy this situation. Given their proven effectiveness in glacial terrains (Fipke et al., 1995), kimberlite indicator mineral reconnaissance surveys in esker sediments, together with a study of ice-flow indicators and the glacial dispersal of distinctive clasts, were conducted in the Saindon-Cambrien corridor, a region of recognized diamondiferous potential (Moorhead et al., 2003). The survey area covers about 120 000 km^2 and lies between parallels 55°N and 57°N and meridians 68°W and 76°W. The reconnaissance survey was conducted mainly in the course of three field seasons (2002, 2003, 2004) and covered eight NTS map sheets: 23-N, 23-M, 33-P, 33-O, 24-C, 24-D, 34-A, and 34-B (Fig. 1). Striae measured in map sheet 33-N were collected during an earlier survey (Parent et Paradis, 1993). The study area includes the Richmond Gulf aulacogen, as well as the Saindon-Cambrien and Mistassini-Lemoyne zones (Moorhead et al., 2000, 2003), which are deeply fractured structural zones of the Archean basement where several outliers of Proterozoic sediments are preserved and whose diamond potential was suggested following a preliminary survey (Parent et al., 2002). In this structural corridor, extending about 500 km along an east–west axis from the Labrador Trough to Hudson Bay, Quaternary glacial episodes are characterized by polyphase glacial dynamics, which likely add to the complexity of glacial dispersal patterns and make their interpretation that much more difficult (Parent et al., 1996). In the eastern part of the corridor, ice-flow and glacial-transport patterns are particularly complex because the main ice divide in northern Quebec underwent significant shifts and reorientations (e.g. Veillette et al., 1999).

This compendium bulletin of the Geo-mapping for Energy and Minerals program provides the opportunity to re-examine and synthesize legacy data sets from previous surficial geology programs and discuss the regional glacial dynamics of a large area of north-central Quebec and the resulting dispersal patterns of distinctive indicator clasts in glacial and glaciofluvial sediments. This paper, which is updated from a previous report (Parent et al., 2004) and includes the laboratory results from the 2004 field season, thus completes our regional survey. The objectives of this paper are 1) to provide a reconstruction of regional ice-sheet dynamics and a new understanding of the history of the Laurentide Ice Sheet in north-central Quebec by using the complete survey area data sets; 2) to expand on the glacial dispersal model presented in Parent et al. (2004) on the basis of composite dispersal trains derived from outliers of the Sakami Formation within the entire survey area; and 3) to update the results of a kimberlite indicator mineral survey in eskers by adding the 2004 data sets in an effort to assess the diamond potential of the region and to evaluate areas for follow-up exploration.

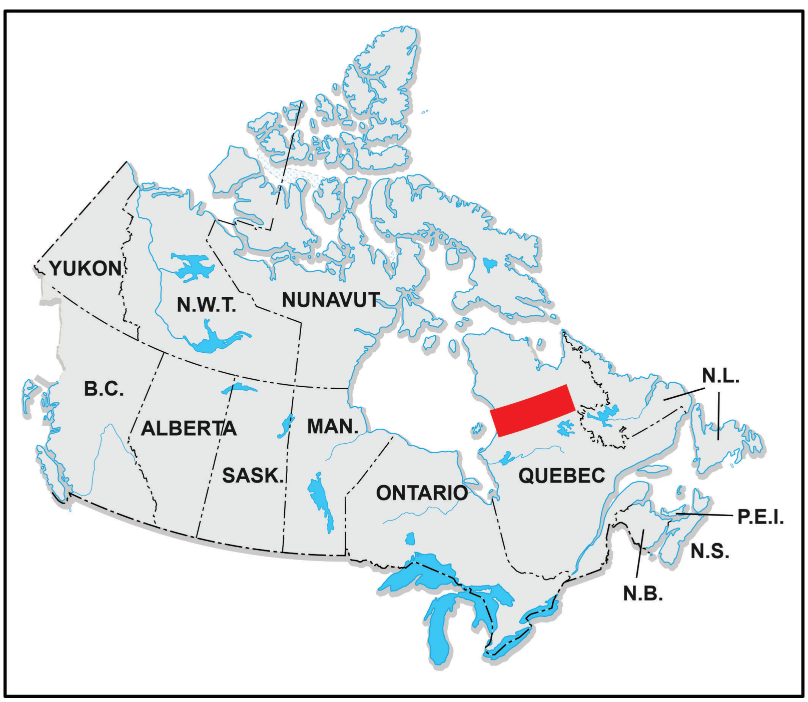

Figure 1. Location of survey region in north-central Quebec.

REGIONAL GLACIAL DYNAMICS

Because the complexity of glacial dispersal patterns is largely governed by regional ice-flow dynamics, particularly the direction, succession, and relative duration of regional glacial movements (Parent et al., 1996), deciphering regional glacial dynamics is a key component of drift prospecting techniques (DiLabio and Coker, 1989). In the Saindon-Cambrien corridor, as in many other areas of northern Canada, establishing the regional prospectivity for diamond exploration rests largely on the presence of kimberlite indicator minerals in glacial or glaciofluvial sediments. The interpretation or follow-up of a regional kimberlite indicator mineral survey thus requires a thorough assessment of regional ice-flow dynamics, along with regional glacial dispersal models.

The presence of multiple successive glacial movements has been recognized since the early 1980s in north-central Quebec (Bouchard and Martineau, 1985; Veillette, 1986; Parent and Paradis, 1993; Parent et al., 1995; Veillette et al., 1999); this succession of glacial movements led to the formation of complex dispersal patterns. It is largely on the basis of work conducted in this region that Parent et al. (1996) discovered and defined palimpsest dispersal trains. In their simplest form, palimpsest dispersal trains are residual trains produced when the lithic components of an earlier dispersal train are incompletely re-entrained by subsequent glacial transport by ice generally moving in a different direction. Polyphase glacial transport and the resulting composite dispersal trains, including palimpsest trains, have now been recognized in many regions of northern Canada (*see* Paulen and McMartin, 2009; Cummings and Russell, 2018; Rice et al., this volume).

In keeping with methodology described in several earlier publications (Veillette, 1986; Lortie and Martineau, 1987; Klassen and Thompson, 1993; Parent et al., 1995; Veillette et al., 1999), striated outcrop surfaces located in sheltered positions relative to the last regional glacial movement were sought out at all landing sites. Such sheltered striated surfaces were found at 61.5% of the 247 outcrops examined during the 2001, 2002, 2003, and 2004 field seasons, a proportion much larger than that attained during our earlier survey (Parent and Paradis, 1993) in map areas 33-O and 33-N. The main reason for this higher percentage is our increased ability to recognize sites favourable to the preservation of multiple ice-flow directions; in addition, we have improved our skills at uncovering sheltered surfaces on igneous and metamorphic rock outcrops characteristic of the local Archean shield terrain. Although the number of observations was not particularly large given the size of the study area, it was sufficiently ample to distinguish four regional-scale glacial phases (Fig. 2), a process favoured by the ease with which the last regional ice movement could be identified on outcrops, as well as on airphotos and satellite images. On the other hand, detecting reliable evidence of earlier ice-flow phases on airphotos or satellite imagery was rarely possible. The ice-flow phases recognized in the region are updated from Parent et al. (2004) and presented in the sections below, where they are discussed from youngest to oldest.

Late-glacial reorientations

The most recent regional glacial phase is associated with a late, though significant, flow reorientation toward the north-northeast that affected the eastern part of the study area (Fig. 2). Unlike striated surfaces associated with the last glacial maximum or with earlier ice-flow phases, striated surfaces recording this late-glacial reorientation mostly consist of striations superimposed (or overprinted) on previously striated surfaces and facets. The flow reorientation consists of a counterclockwise shift of 20° to 40° from the east-northeast ice-flow direction of the previous phase. This set of younger striations can be observed on most outcrops located east of a demarcation line that we interpret as an ice divide that had formed during the previous ice-flow phase and that seems to have migrated very little, if at all, during the late reorientation. At a regional scale, this late-glacial reorientation, inferred to have been initiated by ice streaming into Ungava Bay (Veillette et al., 1999), seemingly caused only minor displacement of the regional ice divide, with the result that the shift of ice-flow direction from east-northeast to north-northeast was moderate in the eastern part of the study area (Fig. 2). At about the same time, that is, about 9000 years BP, the southeastern Hudson Bay region was also affected by reorientation due to glacial streaming toward the southwest (Parent et al., 1995) and ice-stream development to the south in James Bay (Veillette, 1997).

The position of the ice divide shown in Figure 2 is the one recorded at the time of the late-glacial reorientation and coincides with that of the so-called ‘Horseshoe ice divide’, as shown on the Glacial Map of Canada (Prest et al., 1968). Development of this divide has been linked to late-glacial drawdown (Hughes, 1964) and streaming (Veillette et al., 1999) into Ungava Bay. Although this divide appears to have migrated little from the main ice divide during the late-glacial reorientation, glacial dispersal data presented in the next section show that it had previously migrated westward at least 100 km from its position at the last glacial maximum.

Last glacial maximum

Ice-flow directions associated with the last glacial maximum are oriented west-southwest and east-northeast of the main ice divide (Fig. 2); the latter had a roughly northwest–southeast trend and had gradually migrated westward during this protracted glacial phase. Striations produced during this episode can be readily observed on the upper surfaces of most outcrops in the area (Fig. 2). Along the western limb of the regional ice divide, this 260° ice-flow direction is essentially consistent with directions previously documented farther west (Parent et al., 1995) and south (Veillette et al., 1999). Not surprisingly, we believe this westward flow is

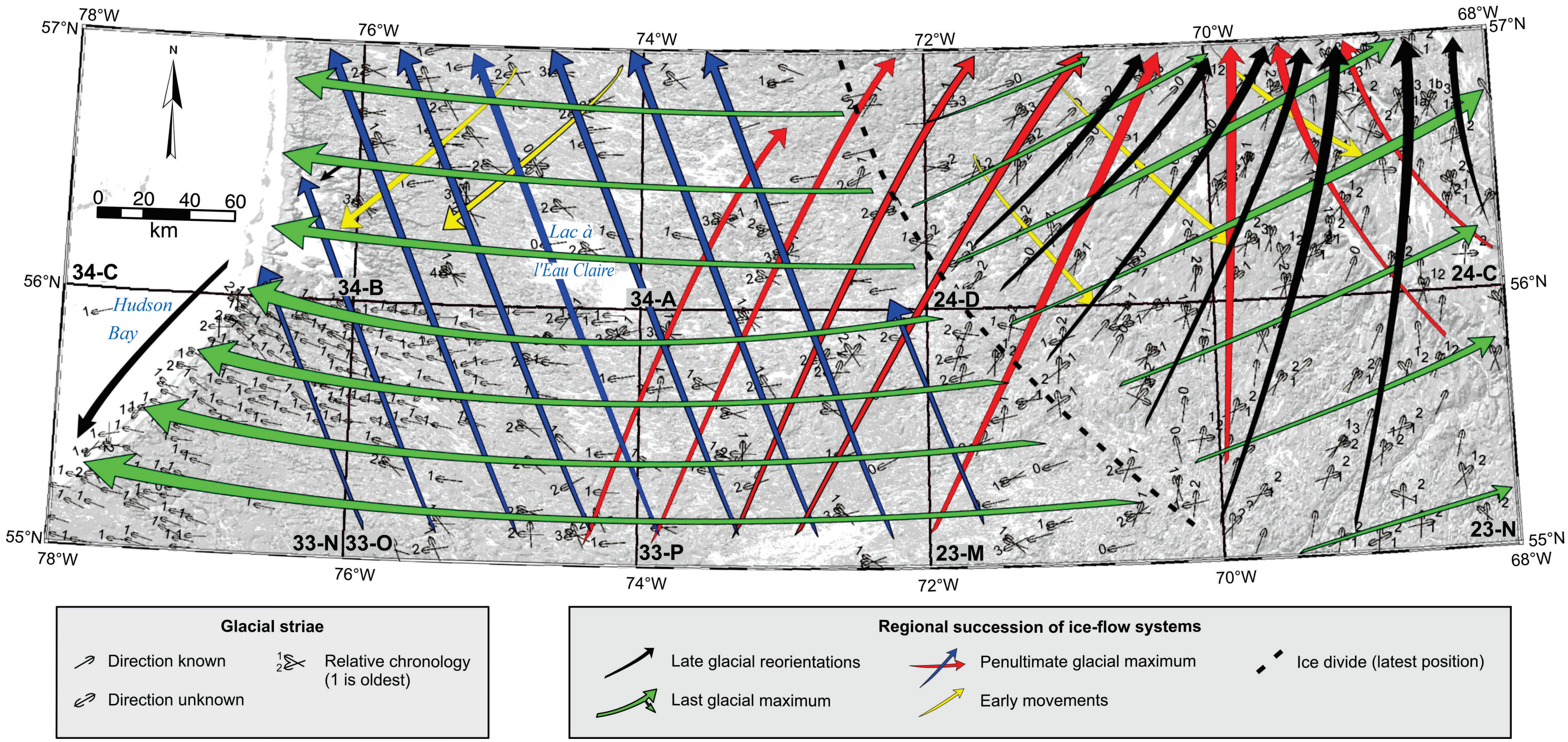

Figure 2. Succession of regional glacial movements in the Saindon-Cambrien corridor of north-central Quebec. Note that the ice divide is shown at its latest position, that is, at the time of late-glacial reorientations (*see also* Fig. 5). *After* Parent et al. (2004, their Fig. 5).

part of the regional southwestward-splaying flow system so characteristic of north-central Quebec and long recognized as the flow system formed during the last glacial maximum (Prest et al., 1968; Shilts, 1980). Prominent west-trending dispersal trains such as those from the Lac à l'Eau Claire impactites (Parent et al., 1995) and from the Lake Fagnant volcanic rocks (Parent et al., 1996), associated with this regional glacial movement, indicate that this is the dominant vector of glacial transport. Although ice-divide migrations can in part be recognized on the basis of glacial striation data, the most diagnostic feature is unquestionably that recorded by the dispersal of distinctive lithic fragments such as those derived from the Sakami Formation; this aspect will be discussed in a following section dedicated to the regional dispersal of this key lithological indicator.

Penultimate glacial maximum

The penultimate glacial maximum is represented by glacial movements directed toward the northwest and the north-northeast, which produced striations observed on a number of sheltered outcrop surfaces in the region (Fig. 2). The very nature of these striated and polished facets and their areal distribution suggest that the ice divide associated with these movements was located much farther south of the region. In the area where both movements were recognized, that is, broadly between 72°W and 74°W, residual surfaces associated with the north-northeast-directed movement clearly predate those associated with the northwest-directed movement, and they are markedly less common. Although the role of these movements in glacial transport and dispersal from sources as small as potential kimberlite pipes has yet to be documented in this region, these movements may very well have led to the formation of composite dispersal trains (Parent et al., 1996) such as those associated with the Sakami Formation outliers, which will be discussed in the next section.

Although the early northwest and north-northeast movements have now been recognized throughout much of north-central Quebec (Parent and Paradis, 1993; Parent et al., 1995, 1996; Veillette et al., 1999; Dubé-Loubert et al., 2021; Rice et al., this volume), their areal extent remains somewhat sketchy. For instance, Veillette et al. (1999) postulated that they do not extend north of Lacs des Loups Marins (56.5°N); however, our surveys (Parent et al., 2003) indicate that they actually extend as far north as Lake Payne (about 59.5°N), over 300 km north of Lacs des Loups Marins. The age of the north-northeast and northwest glacial movements is somewhat conjectural, but the fact that they extend from the vicinity of Lake Mistassini (about 51°N) to that of Lake Payne, a distance of almost 1000 km, indicates that they formed during a major phase of ice-sheet expansion and thus date back to at least the penultimate glacial maximum (e.g. Early Wisconsinan, or Marine Isotope Stage (MIS) 4). Observations of ferromanganese varnish on many northeast-striated surfaces on the shores of hydroelectric reservoirs led Veillette et al. (1999) to propose an older, pre-Wisconsinan age for the northeast movement in north-central Quebec. Because our observations were made on restricted, manually scraped bedrock exposures that are not propitious for recognizing such varnished surfaces, we cannot confirm the interpretation of a pre-Sangamonian age by Veillette et al. (1999). During our surveys, however, we frequently noted the presence of well developed ferromanganese films on bedrock surfaces overlain by podzolic soils developed in shallow sandy tills, which suggests that such varnishes may simply be Holocene in age. This interpretation is also supported by cosmogenic ages that do not show exposure inheritance on outcrops covered by northeast-trending striae in the nearby De Pas River region (Rice et al., 2019).

Early movements

The earliest recorded glacial movements are oriented toward the southwest in the western part of the region and toward the southeast in the eastern part. Erosional features associated with these early movements are relatively scarce; in fact, no striations associated with these movements were observed in the southern half of the study area (Fig. 2), an observation that is also suggested by the absence of southward dispersal from the various outliers of the Sakami Formation (*see* below). The southwest and southeast flow systems, however, are abundantly recorded in regions up to the latitude (59.5°N) of Lake Payne (Parent et al., 2003). These early movements are most likely associated with the development of the Ungava outflow centre (Daigneault and Bouchard, 2004) after the last interglacial. This interpretation finds some support in the positional record of the Ungava ice divide, which generally remained south of the Cape Smith belt (about 61°N), as documented by the limited dispersal of ultramafic indicators from the Cape Smith belt toward the south, in comparison to their important northward transport (Daigneault, 2008).

GLACIAL DISPERSAL OF CLASTS FROM SAKAMI FORMATION OUTLIERS

The Sakami Formation is primarily composed of unmetamorphosed Proterozoic reddish sandstone and orange quartzite, which constitute a very distinctive lithological assemblage exposed in four outliers that contrast sharply with the igneous and metamorphic rocks of the surrounding Archean craton (Fig. 3). Pebbles derived from these outliers are so distinctive that their presence in glacial and glaciofluvial sediments can be easily and confidently established, a task further facilitated by the widespread presence of pebbly pavements at the surface of these glacial and glaciofluvial deposits (caused by aeolian deflation on esker ridges and by mud boil development on till surfaces). It is worth noting that, as the region was the focus of systematic geological

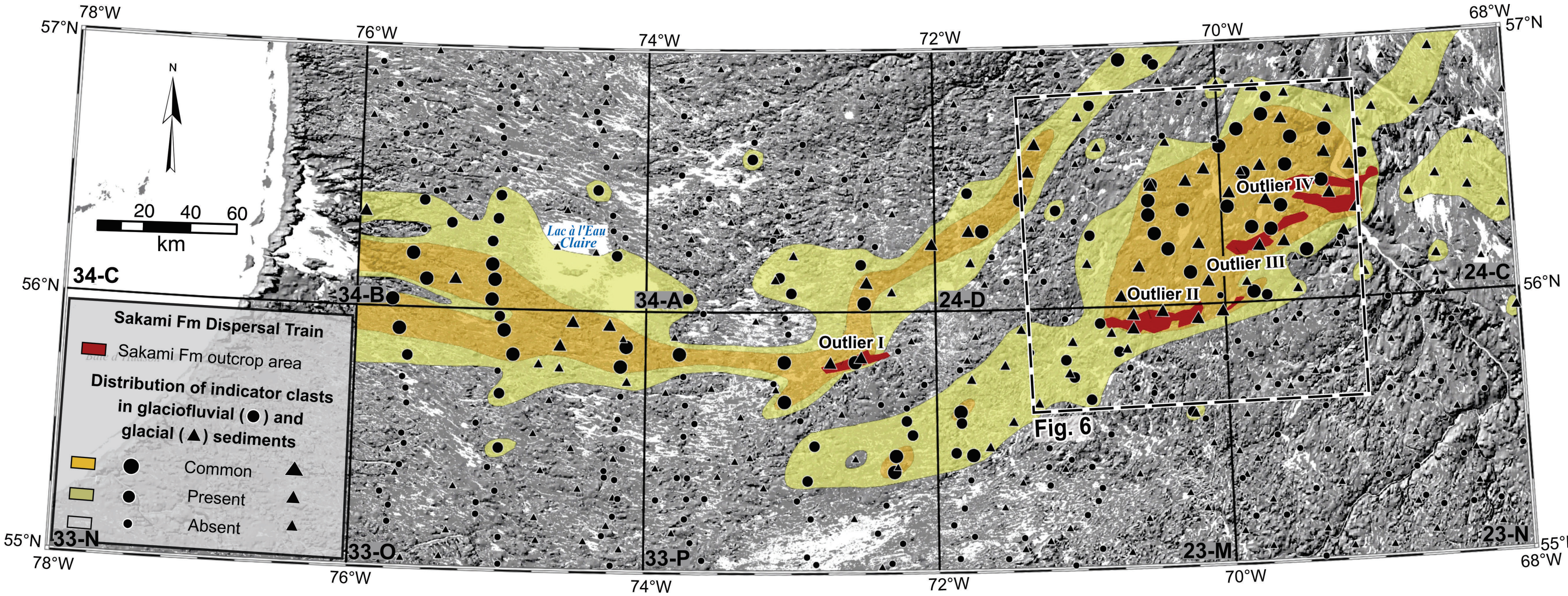

Figure 3. Relative abundance of clasts derived from the Sakami Formation in glacial and glaciofluvial sediments of the Saindon-Cambrien corridor. Note the composite dispersal trains originating from distinct Proterozoic outliers. *See* text and Figure 4 for details. *After* Parent et al. (2004, their Fig. 6).

mapping as part of Quebec's 'Far North' program (Gosselin and Simard, 2000; Gosselin et al., 2001, 2002; Simard et al., 2001) and as the eastern part of the region (map sheets 23-N and 24-C) had been mapped earlier (Dimroth, 1978; Dressler and Ciesielski, 1979), it seems unreasonable to invoke the existence of hypothetically unmapped outcrops to explain the observed dispersal trains (Fig. 3).

Assessing the qualitative abundance of Sakami Formation clasts in glacial and glaciofluvial sediments

In the operational context in which our observations took place, it was too time-consuming to carry out lithological counts in the field; instead, at each observation (landing) site, we simply noted the presence or absence of indicator pebbles by using three qualitative frequency classes (absent, present, common). The mapping of this excellent lithological indicator reveals polyphase drift dispersal patterns that though relatively complex, shed light on regional glacial dynamics and transport. In the context of diamond exploration, the dispersal of these lithological indicators has proved extremely useful, as these outliers happen to be located in the area where several kimberlite indicator minerals were observed (*see* Fig. 6). These lithological indicators are therefore likely to provide at least a preliminary model of regional glacial dispersal. The section below discusses the results of a detailed survey to model glacial transport from outlier II and provides an update of the regional glacial dispersal patterns from Parent et al. (2004).

With the objectives of testing and quantifying our qualitative frequency estimates of Sakami Formation clasts in till, we collected a series of 54 fine gravel samples at the surface of mud boils to carry out pebble counts from surface till. Each sample consisted of about 200 small pebbles (4–16 mm) collected at landing sites spaced at about 10 km intervals (Fig. 4a). This sample set was collected in a grid covering the area around outlier II and extending about 60 km down-glacier (northeast) from the outlier (Fig. 3 and 4). The pebble counts (Fig. 4b) indicate that the 'frequent' frequency class ('FF') averages 25.2% and ranges from 11.2% to 59.2%; the 'common' frequency class ('F') averages 17.33% (n = 17) and ranges from 0% to 67.2%; the 'present' frequency class ('P') averages 4.5% (n = 18) and covers frequencies ranging from 0% to 18.7%; and the 'absent' frequency class averages 0.6% and ranges from 0% to 4.1%. Although there is overlap between the four field-estimated classes, the box and whisker diagram (Fig. 4b) shows that the qualitative field classes display distinctly increasing medians and quartile deviation. Detailed analysis of the pebble counts shows that the class averages and medians are correctly ordered and that only 2 of the 54 samples were really misclassified (one P and one F) and that 4 samples were slightly misclassified (one A, two P, one F). Nonetheless, comparison of Figure 3 and

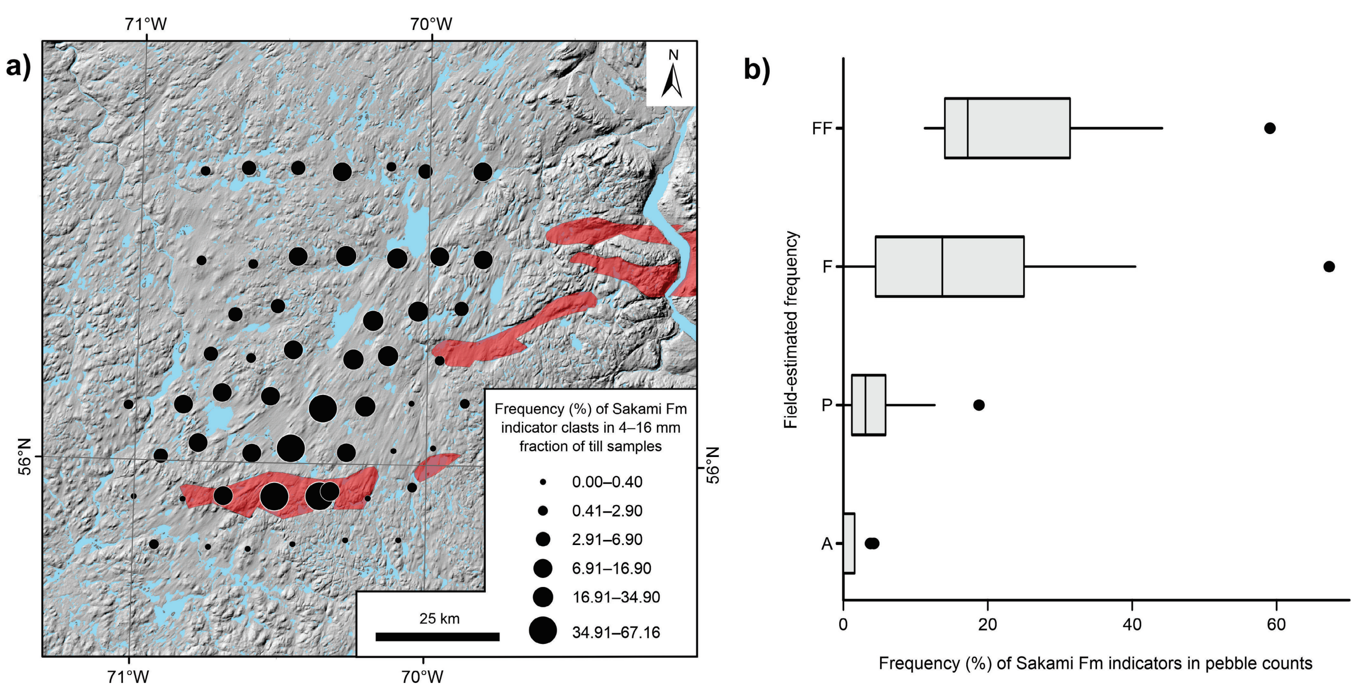

Figure 4. Frequency (%) of Sakami Formation indicator clasts in pebble counts ($n \approx 200$) of the 4 to 16 mm fraction of till samples (n = 54). **a)** Areal distribution of Sakami Formation clasts in till. Note the mega-scale glacial lineation flowset extending northeastward of outlier II (*see* Fig. 3 for outlier nomenclature). **b)** Boxplot comparing semiquantitative classes (A = absent ($\bar{x}$ = 0.6%); P = present ($\bar{x}$ = 4.5%); F = common ($\bar{x}$ = 17.3%); FF = frequent ($\bar{x}$ = 25.2%)) with pebble counts.

Figure 4 confirms the general validity of both the qualitative frequency classes and the regional dispersal patterns shown in Figure 3.

Closer examination of the hill-shaded digital elevation model forming the base map of Figure 4a reveals a conspicuous flowset of mega-scale glacial lineations defining a paleo-ice stream extending northeastward from an onset zone located near outlier II; this small ice stream (15–20 km wide) is believed to be a tributary of the Ungava Bay ice stream (Veillette et al., 1999; Margold et al., 2018).

The areal distribution of pebbles derived from the four outliers of the Sakami Formation in glacial and glaciofluvial sediments of the region (Fig. 3) clearly shows that 1) distinctive indicator clasts can be traced over hundreds of kilometres in the midst of the Archean craton of north-central Quebec, the core region of one of the major dispersal centres of the Laurentide Ice Sheet (Shilts, 1980; Prest, 1984); and that 2) the polyphase dispersal trains derived from the four outliers provide unique information on regional glacial dynamics (Fig. 5). For the purposes of our analysis, the four outliers of the Sakami Formation are simply identified from west to east as outliers I, II, III, and IV (Fig. 3).

Because outlier I is about 90 km west of the outlier II, III, and IV group, its dispersal patterns can be readily distinguished from those derived from the other outliers. Figure 3 shows that the dispersal pattern from outlier I consists of two major dispersal trains: one that is broadly fan-shaped (an indicator of palimpsest dispersal; *see* Parent et al., 1995, 1996) and extends westward over a distance of at least 200 km; and one that is ribbon-shaped and extends northeast over a distance of as much as 150 km. Although these dispersal trains were obviously emplaced as a result of the last glacial movements, which were directed in almost opposite directions in the region (broadly west and northeast; Fig. 2, 5d, 5e), the presence of palimpsest components, such as a low-concentration 'blob' about 30 km north of outlier I, is also obvious. Hence, our reconstruction of the dispersal patterns of Sakami Formation clasts is based on the conceptual model of palimpsest dispersal (Parent et al., 1996). Taking into account the ice-flow directions and chronology recognized in the region, our reconstruction proposes that clasts originating from outlier I were first dispersed toward the north-northeast, then toward the northwest over a traceable distance of some 60 km during the penultimate glacial maximum (Fig. 5a, b). Subsequently, presumably during the last glacial maximum, Sakami Formation clasts were dispersed westward from outliers I and II, while clasts previously dispersed toward the northeast and northwest were re-entrained toward the west (Fig. 5c). During that phase of clastic dispersal, the main ice divide had to be located well east of outlier II to allow the dispersal of its clasts toward the west over a distance of some 150 km.

During a subsequent phase of the last glacial maximum, the westward migration of the ice divide led to a shutdown of all westward clast dispersal and of re-entrainment from outliers II, III, and IV (Fig. 5d). However, during this flow episode, westward dispersal and re-entrainment from outlier I continued, reaching at least 200 km, beyond the limit of our study area. During this ice-flow episode, clasts from outliers II, III, and IV were dispersed or re-entrained toward the northeast (Fig. 5d). During the last regional glacial phase (Fig. 5e), a long ribbon-shaped train formed northeast of outlier I, and previously transported clasts were re-entrained over smooth, mega-scale glacial lineation covered terrain by ice streaming toward Ungava Bay. Figure 3 suggests that the re-entrainment of indicator clasts was weaker over the hilly terrains northeast of outliers III and IV during this late-glacial phase. As observed in Figure 4a, strong northeastward dispersal from outlier II took place in a second mega-scale glacial lineation corridor, which we interpret as the footprint of another tributary ice stream.

Migration of the regional ice divide during the last glaciation

As the latest position of the ice divide is located between outlier I and the outliers II, III, and IV group, the westward dispersal of indicators from the latter group necessarily took place during an earlier glacial phase, either during an early last glacial maximum phase (Fig. 5c) or during a later last glacial maximum phase (Fig. 5d). As shown in Figure 5, our preference goes to the early last glacial maximum option, as this interpretation seems more consistent with the general weakness of eastward dispersal from outliers II, III, and IV (Fig. 3). Furthermore, this interpretation provides an explanation for the differential length of westward dispersal trains derived from outliers I and II; the dispersal train west-southwest of outlier II is 150 km long, whereas the train derived from outlier I is at least 200 km long and may extend farther west into Hudson Bay.

Our reconstruction of the regional ice divide indicates that it migrated from the vicinity of outliers III and IV to halfway between outliers I and II (Fig. 5c, d, e), a distance of about 150 km. This latest position of the regional ice divide at about longitude 70°W appears as the northern continuation of the major divide identified by Klassen and Thompson (1993, ice-flow event II in their Fig. 27) in central Labrador. It also coincides roughly with the western arm of the Ancestral Labrador Ice Divide during the last glacial maximum (Dyke and Prest, 1987); however, the two-pronged nature of the Ancestral Labrador Ice Divide during and after the last glacial maximum was abandoned in a subsequent assessment (Veillette et al., 1999) but was re-introduced more recently by Rice et al. (2019, 2020) and Dubé-Loubert et al. (2021, their Fig. 9). Although some doubts concerning the eastern Ancestral Labrador Ice Divide may be justified, notably because of the difficulty in identifying it in areas where its development may coincide with that of the late-glacial Horseshoe ice divide (Veillette et al., 1999; Dubé-Loubert et al., 2021), this difficulty is resolved in the area of the western Ancestral Labrador Ice Divide, where glacial dispersal

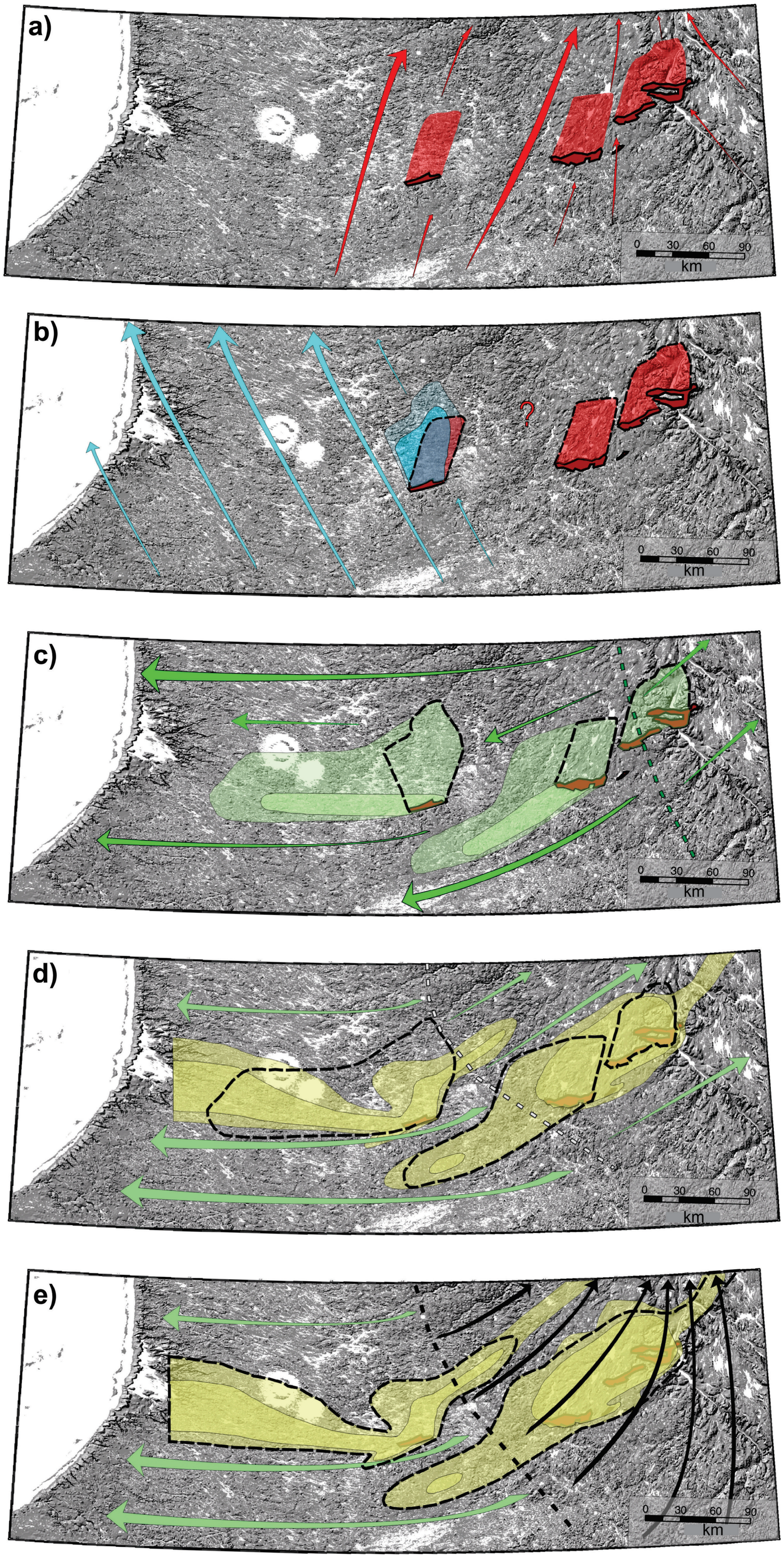

Figure 5. Succession of glacial movements and polyphase dispersal of clasts derived from the Sakami Formation, north-central Quebec. From oldest to youngest: **a)** penultimate glacial maximum I, **b)** penultimate glacial maximum II, **c)** last glacial maximum I, **d)** last glacial maximum II, and **e)** deglaciation. Dashed lines indicate successive positions of the ice divide. *After* Parent et al. (2004, their Fig. 7).

data reported herein provide indisputable evidence of not only the position and orientation of the divide but also of its migration during the last glaciation (Fig. 2 and 5c; *see also* Klassen and Thompson, 1993).

The role of ice streaming during deglaciation

As shown in Figure 4a, the hill-shaded digital elevation model derived from the Shuttle Radar Topography Mission data set (USGS, 2008) enables us to identify mega-scale glacial lineation corridors defining tracts of fast-flowing ice that we interpret as the footprint of paleo-ice streams. In the study area, we identified two distinct mega-scale glacial lineation corridors: one is located northeast of outlier II (Fig. 4), and the other one extends northeastward of outlier I and is delineated by a 150 km long dispersal train of Sakami Formation indicators (Fig. 3). This ribbon-shaped dispersal train presumably records the late-glacial reorientation toward the northeast, which is the last major ice-flow event that affected this part of the region (Fig. 5e). As the fast ice-flow corridor starts near the position of the Horseshoe ice divide and therefore does not reach outlier I (Fig. 5e), we infer that this dispersal train formed mainly as a result of re-entrainment of Sakami Formation clasts that had been transported northward during the penultimate glacial maximum phase. Given the short duration generally inferred for the late-glacial flow reorientation (Margold et al., 2018; Dubé-Loubert et al., 2021) and the considerable length of the ribbon-shaped dispersal train, we believe that the dispersal train records a narrow zone of fast-flowing ice, presumably a second tributary ice stream connecting with the major ice stream that formed in western Ungava Bay (Veillette et al., 1999; Margold et al., 2018).

KIMBERLITE INDICATOR MINERAL SURVEY

This section on the kimberlite indicator mineral survey in the Saindon-Cambrien corridor is essentially derived from Parent et al. (2004), but with the addition of the 2004 data sets collected in NTS 23-N and 24-C. The results and interpretations remain essentially the same, except for a few additions to Figure 7.

Methodology

A total of 268 samples were collected during the kimberlite indicator mineral survey of the Saindon-Cambrien structural zone, most of which (225) were collected in cobbly and pebbly esker sediments to take advantage of the strong hydraulic sorting taking place naturally in subglacial tunnels (Fig. 6). Completing the regional coverage of the survey required that other surficial media be sampled: six samples were collected in other glaciofluvial sediments, such as outwash plains (n = 2), undifferentiated ice-contact sediments (n = 2), and glaciomarine deltas (n = 2). The remaining 37 samples consisted of till collected in areas such as NTS 23-N, where glaciofluvial sediment bodies, particularly eskers, are too scarce or too small to be readily identified on satellite imagery or during helicopter traverses.

The samples were dry-sieved in the field until about 20 kg of material finer than 4.0 mm in diameter was recovered. These samples were then submitted to standard processing: 1) pre-concentration on a Wilfley shaker table; 2) heavy mineral concentration in a sodium polytungstate solution (brought by evaporation to a specific gravity of 3.2); 3) paramagnetic separation; and 4) microscopic identification in a commercial laboratory (IOS Services Géoscientifiques Inc.), which was also responsible for picking and mounting indicator mineral grains for microprobe analysis at Université Laval. Only kimberlite indicator minerals confirmed by microprobe analyses are mapped in Figure 6. Analytical results for picroilmenites, magnesian chromites, mantle diopsides, and eclogitic garnets are listed in Table 1 and plotted in Figure 7a, b, c, d, and e.

Regional distribution of kimberlite indicator minerals

Surveys conducted in the Saindon-Cambrien corridor study area led to the identification of several new kimberlite indicator minerals, including 12 picroilmenite grains, 4 magnesian chromite grains, 1 eclogitic garnet grain (G3), and 3 mantle diopside grains from the diamond inclusion window, in addition to the 4 picroilmenite grains previously identified in our preliminary 2001 survey (Parent et al., 2002). This new suite of indicator minerals comes in the wake of previous reports by BHP of G9 pyropes, picroilmenites, chrome diopsides, and a perovskite grain in the region (Girard, 1999; Beaumier, 2002). In 2004, fieldwork was concentrated in the easternmost part of the Saindon-Cambrien structural zone where it intersects the Mistassini-Lemoyne structural zone (Fig. 6).

In addition to peridotitic pyropes (G9 and G10 garnets), chrome picroilmenites, magnesian chromites, and certain peridotitic diopsides (chrome-rich) are among the most characteristic kimberlitic minerals and the most widely used in diamond exploration (Gurney and Zweistra, 1995). Indicator minerals discovered in the course of our surveys are therefore significant for diamond exploration in the study area. This low-density regional survey carried out between 2001 and 2004 constitutes a first step toward assessing the diamond potential of the Saindon-Cambrien and Richmond Gulf structural zones.

Indicator minerals recognized in this survey are distributed along two nearly perpendicular corridors that intersect in the eastern part of the study area (Fig. 6). The first corridor, roughly 100 km wide, trends east–west across the Lake Bienville (33-P) and Lake Gayot (23-M) map sheets. The second corridor, about 75 km wide, extends along a

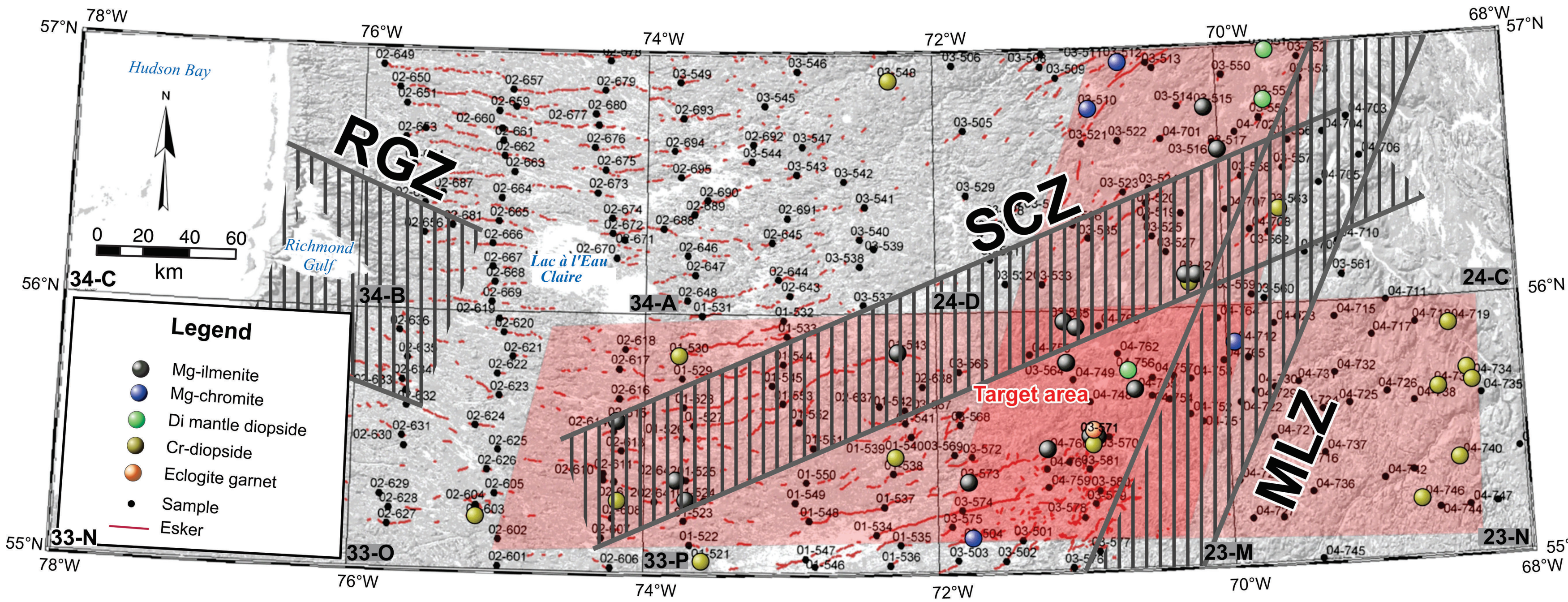

Figure 6. Distribution of kimberlite indicator minerals in esker sediments of the Saindon-Cambrien structural zone, north-central Quebec. Samples with no kimberlite indicator minerals are indicated by a black dot. Indicator minerals identified so far are distributed along two corridors (shown in pink). Note the concentration of kimberlite indicator minerals in NTS map area 23-M ('target area'). Structural zones are delineated by grey diagonal stripes and labelled RGZ (Richmond Gulf zone), SCZ (Saindon-Cambrien zone), and MLZ (Mistassini-Lemoyne zone).

Table 1. Analyses of kimberlite indicator minerals found in eskers in the Saindon-Cambrien structural zone, north-central Quebec.

Picroilmenites																			
Sample #	**UTM zone**	**Easting**	**Northing**	**SiO_2**	**TiO_2**	**Al_2O_3**	**Cr_2O_3**	**Fe_2O_3**	**MgO**	**MnO**	**FeO**	**Na_2O**	**Nb_2O_3**	**ZnO**		**Total**			
03-515	19	433238	6292123	0.04	48.70	0.51	1.05	14.03	10.01	0.23	26.57	0.02	0.15	0.02		101.34		Kimberlitic	
03-517	19	438335	6273877	0.01	49.41	0.47	1.00	12.57	10.03	0.24	27.11	0.05	0.17	0.00		101.05		Kimberlitic	
03-526	19	423020	6220539	0.02	48.59	0.53	0.92	14.28	9.85	0.24	26.71	0.04	0.11	0.00		101.29		Kimberlitic	
03-526	19	423020	6220539	0.04	49.68	0.48	0.81	12.22	10.26	0.19	26.92	0.02	0.17	0.00		100.79		Kimberlitic	
03-564	19	367523	6185719	0.02	51.73	0.23	0.36	10.19	11.32	0.23	26.44	0.01	0.25	0.00		100.78		Kimberlitic	
03-565	19	367982	6203414	0.04	49.68	0.43	1.04	12.69	10.35	0.23	26.79	0.02	0.17	0.03		101.46		Kimberlitic	
03-565	19	367982	6203414	0.05	51.05	0.44	1.54	9.37	11.61	0.29	25.97	0.05	0.17	0.03		100.57		Kimberlitic	
03-571	19	376347	6153185	0.05	46.42	0.55	0.49	17.20	8.26	0.18	27.47	0.00	0.20	0.00		100.80		Kimberlitic	
03-571	19	376347	6153185	0.02	46.58	0.50	0.45	17.07	8.30	0.24	27.40	0.04	0.22	0.05		100.87		Kimberlitic	
03-573	19	323663	6136549	0.02	50.66	0.41	2.38	9.37	11.99	0.20	25.40	0.02	0.20	0.00		100.64		Kimberlitic	
01-524	19	581872	6126256	0.03	48.23	0.52	0.94	24.41	9.92	0.24	15.54	0.03	0.23			100.11		Kimberlitic	
01-543	19	671207	6192416	0.07	48.15	0.53	0.68	25.36	9.54	0.27	16.44	0.06	0.19			101.28		Kimberlitic	
04-755	19	397278	6171979	0.042	48.36	0.556	0.962	13.46	10.1	0.173	26.16	0.024	0.18	0.039		100.1		Kimberlitic	
04-760	19	357991	6148403	0.039	49.08	0.471	0.828	12.89	10.82	0.235	25.34	0.054	0.204	0		99.95		Kimberlitic	
#		UTME	UTMN	SiO_2	TiO_2	Al_2O_3	Cr_2O_3	Fe_2O_3	MgO	MnO	FeO	Na_2O	Nb_2O_3	ZnO	CaO	Total			
02-615	18	551382	6159762	0.04	47.64	0.46	0.66	15.00	9.93	0.22	25.56	0.02		0.00	0.02	99.54		Kimberlitic	
02-642	18	577538	6135314	0.03	45.45	0.55	0.89	17.24	9.71	0.20	24.15	0.03		0.00	0.01	98.25		Kimberlitic	
Magnesian chromites																		**CALCULATED**	
#		Easting	Northing	SiO_2	TiO_2	Al_2O_3	Cr_2O_3	Fe_2O_3	MgO	MnO	FeO	Na_2O	Nb_2O_3	ZnO	Total	Fe_2O_3	FeO	FeO_{tot}	Total
03-510	19	383518	6294484	0.05	1.53	11.83	55.31	7.63	14.01	0.00	10.88	0.03	0.01	0.14	101.4	4.15	14.01	17.74	101.07
03-511	19	397165	6313482	0.02	0.39	21.98	47.82	2.67	12.95	0.00	15.36	0.01	0.00	0.15	101.3	1.62	16.31	17.76	101.24
03-504	19	323880	6112174	0.02	0.23	11.63	48.88	16.89	10.00	0.00	13.69	0.00	0.00	0.20	101.5	11.23	18.78	28.88	100.95
04-712	19	441517	6189748	0.00	0.51	22.20	37.24	14.17	9.71	0.00	16.41	0.005	0.00	0.15	100.4	29.15	19.81	8.73	98.352172
Mantle diopsides																			
#	Zone	Easting	Northing	SiO_2	TiO_2	Al_2O_3	Cr_2O_3	Fe_2O_3	MgO	MnO	FeO	Na_2O	K_2O	CaO		Total			
03-551	19	458801	6315488	54.93	0.15	1.45	0.75	0.00	17.31	0.04	3.34	1.33	0.02	19.72		99.04		Kimberlitic	
03-554	19	459485	6294009	54.67	0.16	1.52	0.82	0.00	17.63	0.06	3.28	1.37	0.03	18.82		98.35		Kimberlitic	
04-756	19	394812	6180882	55.28	0.18	1.48	0.69	1.16	16.86	0.09	2.55	1.39	0.03	21.12		100.8		Kosmochlor	
Eclogitic garnet																			
#		Easting	Northing	SiO_2	TiO_2	Al_2O_3	Cr_2O_3	Fe_2O_3	MgO	MnO	FeO	Na_2O	CaO			Total			
03-565	19	367982	6203414	36.48	0.04	21.32	0	0	0.76	0.57	24	0.01	15.25			98.43		G3 eclogitic	

Microprobe analyses were carried out by the Laboratoire de microanalyse in the geology department of Université Laval. All analytical results are expressed in percentages. *After* Parent et al. (2004, their Table 1).

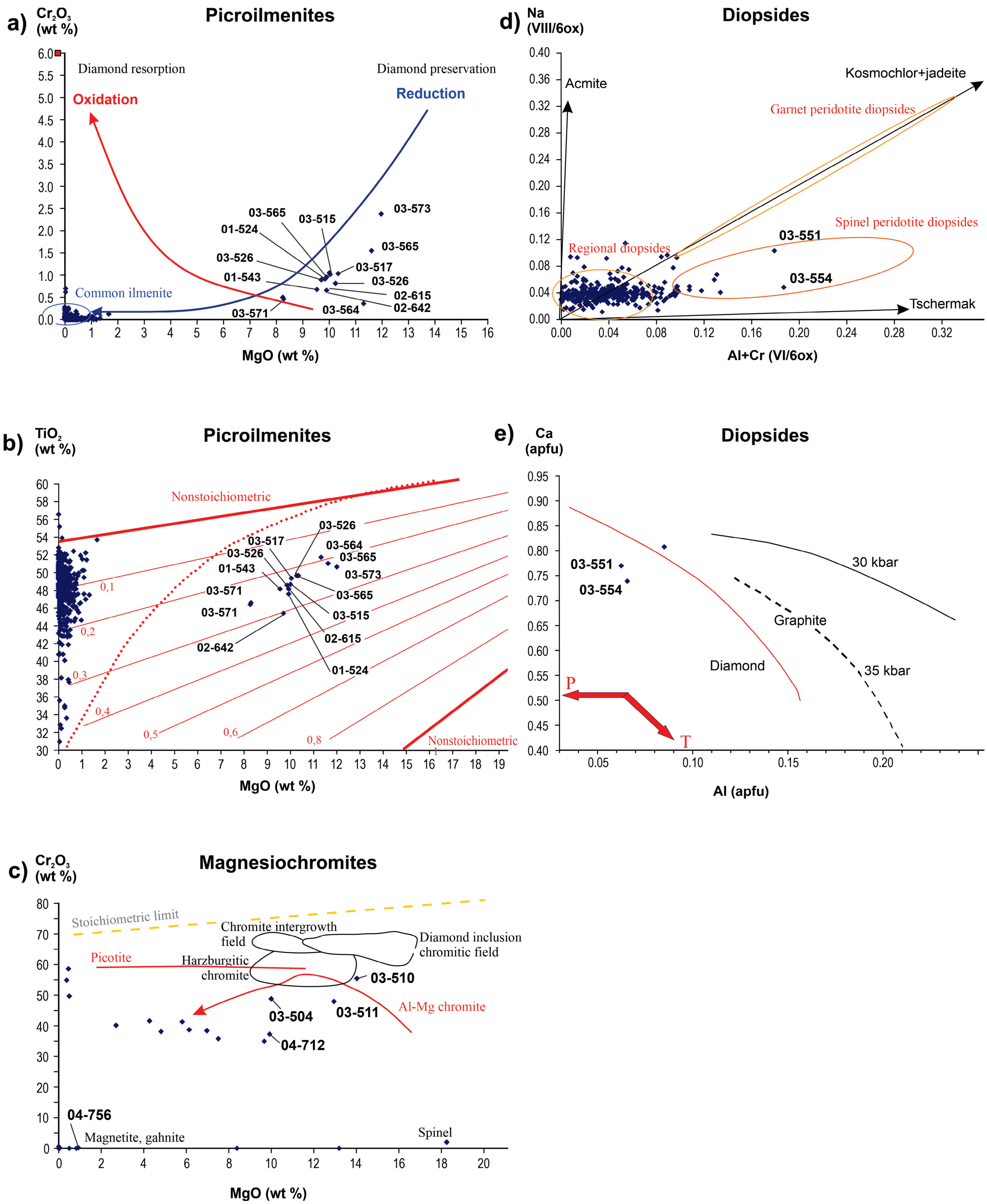
a)
Cr_2O_3 (wt %)
Picroilmenites
Diamond resorption
Diamond preservation
Oxidation
Reduction
Common ilmenite
03-573
03-565
03-515
01-524
03-565
03-526
03-517
01-543
03-526
02-615
02-642
03-571
03-564
MgO (wt %)
d)
Na (VIII/6ox)
Diopsides
Acmite
Kosmochlor+jadeite
Garnet peridotite diopsides
Spinel peridotite diopsides
03-551
Regional diopsides
03-554
Tschermak
Al+Cr (VI/6ox)
b)
TiO_2 (wt %)
Picroilmenites
Nonstoichiometric
03-526
03-517
03-564
03-526
03-565
01-543
03-573
0,1
03-571
03-565
03-571
03-515
0,2
02-615
02-642
0,3
01-524
0,4
0,5
0,6
0,8
Nonstoichiometric
MgO (wt %)
e)
Ca (apfu)
Diopsides
03-551
03-554
30 kbar
Graphite
Diamond
35 kbar
P
T
Al (apfu)
c)
Cr_2O_3 (wt %)
Magnesiochromites
Stoichiometric limit
Chromite intergrowth field
Diamond inclusion chromitic field
Picotite
Harzburgitic chromite
03-510
Al-Mg chromite
03-504
03-511
04-712
04-756
Magnetite, gahnite
Spinel
MgO (wt %)

Figure 7. Analytical plots of kimberlite indicator mineral grains retrieved from esker samples in the Saindon-Cambrien structural zone, north-central Quebec. **a)** Chromium vs. magnesium concentrations in picroilmenite grains (*original modified from* Gurney and Moore, 1993). Note the correlation between the analyses suggesting a reducing environment. *After* Parent et al. (2004, their Fig. 2b). **b)** Titanium vs. magnesium concentrations in picroilmenite grains (*original modified from* Baumgartner et al., 2003). Note that the results group in the field of macrocrystic ilmenites of kimberlitic origin (below red dashed line). *After* Parent et al. (2004, their Fig. 2a). **c)** Chromium vs. magnesium concentrations in magnesiochromite grains (*original modified from* C.F. Mineral Research Ltd., 1989). Note that three grains plot close to the field of harzburgitic chromites, thus suggesting a mantle origin. *After* Parent et al. (2004, their Fig. 3). **d)** Sobolev diagram (Sobolev, 1974) showing the presence of kosmochlor and jadeite in several grains, suggesting that these come from garnet peridotites at great depth. *After* Parent et al. (2004, their Fig. 4a). **e)** Nimis and Taylor (2000) diagram suggesting pressure–temperature conditions of diopsides from garnet peridotites. Two grains are compatible with the diamond stability field. *After* Parent et al. (2004, their Fig. 4b).

north-northeast–south-southwest axis across the Lake Maricourt (24-D) and Lake Gayot (23-M) map sheets. These directions correspond to regional fracture sets reported by Moorhead et al. (2003), as well as to the regional dispersal trains documented herein (Fig. 3).

Picroilmenites

Picroilmenite grains are widely distributed in the two corridors, but they are more commonly encountered within their intersection zone in map sheet 23-M, where two samples contain two picroilmenite grains each (03-565 and 03-571). Sample 03-571 also contains one eclogitic garnet grain (G3). The magnesium and chrome concentration of these ilmenite grains (Fig. 7a, b and Table 1) is typical of mantle-derived ilmenites (Mitchell, 1986). On the diagram showing the titanium versus magnesium content (Fig. 7b, *modified after* Baumgartner et al., 2003), these analyses clearly plot in the field of kimberlitic macrocrysts. On the diagram showing chromium versus magnesium, commonly used by industry (Fig. 7a, *modified after* Gurney and Moore, 1993), picroilmenite grains show a correlative variation, which is usually attributed to reducing conditions, favourable for diamond preservation.

Magnesian chromites

Several chromite grains were recovered in the present survey. Although the vast majority of these grains show iron enrichment vectors typical of crustal provenance, a few grains stand out: these consist of aluminomagnesian chromites of probable mantle derivation. These magnesian chromite grains were discovered in two areas relatively far from each other: two samples (03-510 and 03-511) were located near Lake Desbergères (24-D), whereas the others (03-504 and 04-712) were located at separate sites near the margins of the intersection zone of the east–west and south-southwest–north-northeast corridors (map area 23-C). Their high chrome content (Fig. 7c), comparable to that of chromite from various diamond-bearing kimberlite occurrences, indicates a deep mantle origin.

Diamond-inclusion mantle diopsides

Diopside grains are quite abundant in the study area; however, discriminating between kimberlitic minerals and crustal minerals is not an easy task. Three grains attracted our attention because their composition suggests they are from a mantle garnet peridotite facies (Fig. 7d). The chemical composition of two of these grains suggests their growth took place in pressure–temperature conditions compatible with those of the diamond stability field (Fig. 7e). They were found at two nearby sample sites (03-551 and 03-554), near Lake Methuselah in the northwestern corner of map area 24-C (Fig. 6).

A number of other diopside grains have compositions suggesting they are derived from spinel peridotite, an upper mantle facies (Fig. 7d). About 10 Cr-diopside grains were identified in the survey area. Except for one sample (03-548), these Cr-diopsides were fairly evenly distributed in the two corridors shown in Figure 6. Numerous (31) diopside grains slightly enriched in chromium (≤1.0%) were recovered from widely scattered samples (see Parent et al., 2004, their Table 2); their significance in diamond exploration seems low. Hence, Cr-diopsides and low-Cr-diopsides are not listed in Table 1.

Garnets

One garnet grain, most likely eclogitic in composition (Table 1), was recovered from sample 03-571 (map sheet 23-M), in which it occurs together with picroilmenite and Cr-diopside grains (Fig. 6). Its significance is difficult to establish at present. Although peridotitic pyrope grains were not recovered in the present survey, G9 garnets were reported in a till survey conducted for a private firm in the region (Girard, 1999; Beaumier, 2002).

DISCUSSION

Prevalence of warm-based conditions

Although Kleman and Glasser (2007) concluded that frozen-bed conditions prevailed in the core region of the Laurentide Ice Sheet on the basis of their assessment of its bed landform record, this study indicates that basal sliding and erosion were active almost continuously during much of the last glaciation in this core region of the eastern Laurentide Ice Sheet. Protracted warm-based conditions are required for basal erosion and debris entrainment to take place on a scale such as that shown by the Sakami Formation composite dispersal train from outlier I. Together with the occurrence of crosscutting striations throughout this region and many other regions in north-central Quebec and Labrador (Klassen and Thompson, 1993; Parent et al., 1995; Veillette et al., 1999; Rice et al., 2019, 2020, this volume; Dubé-Loubert et al., 2021), the observed composite dispersal train indicates that warm-based conditions prevailed not only in its source region but also in adjacent regions. The formation of palimpsest dispersal trains such as shown by the successive phases depicted in Figure 5 (*see also* Parent et al., 1996) implies that subglacial entrainment, and consequently, warm-based conditions, prevailed during most if not all of the last glaciation, a conclusion that is supported by thermomechanical modelling (Marshall and Clark, 2002). The 200 km length of the west-trending ribbon-shaped Sakami dispersal train further confirms the long duration of warm-based conditions in the eastern Laurentide Ice Sheet. The presence of north-northeast- and northwest-trending glacial striae that appear to have formed prior to the last glacial maximum, together with the general thinness of the till cover, suggests that erosion rates were relatively low in north-central Quebec, a conclusion that is also supported by numerical modelling of subglacial erosion and sediment transport (Melanson et al., 2013). Although a largely warm-based landscape is suggested by preservation of glacial landforms and complex dispersal trains along the Quebec–Labrador boundary to the east, those landforms and dispersal trains have been explained by changes in subglacial dynamic and thermal conditions resulting from ice-divide migration (Rice et al., this volume).

This large ribbon-shaped dispersal train also provides an opportunity to assess somewhat independently the temporal framework of our proposed reconstruction (Fig. 5). Realistic flow rates of 1 to 10 m/year, estimated from balanced velocities of the eastern Antarctic Ice Sheet (Bamber et al., 2000; Rignot et al., 2011), suggest that the observed 200 km transport would require anywhere from 20 000 to 200 000 years. Because particles are retarded relative to ice velocities in the subglacial environment and because empirical modelling has shown that key factors in the formation of dispersal trains are travel distance (hence, time × velocity) of basal ice and subglacial debris re-entrainment (Parent et al., 1996), the formation of large dispersal trains such as the Sakami may be estimated to span a period ranging from as little as 20 000 years to as much as 100 000 years (i.e. a full glacial cycle). On that basis and with the knowledge that the Quebec–Labrador peninsula was glaciated from at least early MIS 4 (71 000 to 57 000 years BP), as proposed by Marshall and Clark (2002) and Allard et al. (2012), and that the northeastward and northwestward palimpsest components (Fig. 5a, b) presumably formed during that period, we infer that the formation of the ribbon-shaped dispersal train (Fig. 5c, d) spans most of the last glaciation, that is, MIS 2 (29 000 to 11 700 years BP), and probably includes a major part of MIS 3 (57 000 to 29 000 years BP). As discussed earlier, formation of the long dispersal train extending northeastward from outlier I (Fig. 5e) is associated with ice streaming into Ungava Bay at the time of deglaciation.

Transport distance in glacial and glaciofluvial sediments in subglacial environments

Although this study was not designed to compare transport distances in glacial and glaciofluvial environments, its design was based on previous studies suggesting that esker clasts are primarily re-entrained from nearby glacial sediments (Bolduc, 1992; Levasseur and Prichonnet, 1995). Whether the studied eskers are considered as having formed either in short subglacial conduits or in long conduits, the transport distances in eskers observed by these authors are only a few kilometres longer than in adjacent till, much as Gillberg (1968) had observed earlier. Renewed interest in clastic transport in glaciofluvial systems, particularly in eskers, came in the wake of the discovery of the first Canadian diamond mine (Fipke et al., 1995) through the tracing of kimberlite indicator minerals in an esker system over a distance of 800 km from their source area near Lac de Gras, Northwest Territories.

As shown in this investigation and in an earlier preliminary report (Parent et al., 2002), the dispersal of Sakami Formation indicators (Fig. 5) is generally comparable in terms of distance between eskers and tills, which globally supports the conclusions reached in earlier investigations (Gillberg, 1968; Bolduc, 1992; Levasseur and Prichonnet, 1995). These conclusions are further supported by recent work near Great Slave Lake by Sharpe et al. (2017), who found that clastic dispersal trains extend over 150 km in both esker and till sample sets and that dispersal trains in eskers are only slightly longer (5–25 km) than those in till.

Implications for diamond exploration in the Sakami-Cambrien corridor

The east–west and north-northeast–south-southwest zones in which the presence of kimberlite indicator minerals is recorded (Fig. 6) correspond to the main regional glacial dispersal directions (Fig. 2, 3, 5), which raises the question of whether these two dispersal zones are mainly the result of structural controls, namely, the Saindon-Cambrien and Mistassini-Lemoyne structural zones, or whether they formed mainly as a result of polyphase glacial transport from a single 'target zone' possibly located in the Lake Gayot map area (23-M). An answer to this question requires that follow-up kimberlite indicator mineral surveys be conducted in the Lake Gayot region. Such a follow-up program may now take advantage of the regional dispersal model presented earlier (Fig. 2–5). In any event, the present reconnaissance survey of kimberlite indicator minerals in glaciofluvial sediments demonstrates its efficiency at a relatively low cost. Most importantly, this survey confirms the prospectivity of this region for diamond exploration.

CONCLUSION

A glacial dispersal model based on a series of shifting ice-flow directions and complex dispersal patterns is proposed for the region. This model is grounded on the dispersal of very distinctive lithological markers, red sandstone and orange quartzite clasts, in glaciofluvial and glacial sediments. These indicator clasts are derived from a cluster of outliers of the Sakami Formation, which, though much larger and more prominent, constitute a satisfactory analogue for kimberlite clusters. The most interesting aspect of the reconstructed dispersal trains is a composite train showing that clasts derived from the westernmost outlier (outlier I), located in the upper valley of the Little Baleine River (33-P/16), were successively dispersed in four successive ice-flow directions: toward the north-northeast, the northwest, the west-southwest, and lastly toward the northeast. This composite dispersal train consists of a prominent, 200 km long ribbon-shaped train toward the west-southwest and a palimpsest train caused by the westward re-entrainment of dispersal trains formed by the earlier flows toward the north-northeast and the northwest. The final late-glacial flow reorientation, toward the northeast, also produced a ribbon-shaped train over a distance of at least 150 km, but in a direction almost diametrically opposed to that of the ribbon-shaped trains formed by the earlier flow toward the west-southwest. The colocation of this dispersal train with a belt of mega-scale glacial lineations indicates that ice streaming toward Ungava Bay played a key role in its formation.

Although dispersal patterns derived from outlier II, located near the Lac de la Bouteille outlier (23-M/15, 16), share many of the features associated with those from outlier I, they also show that west-southwest-directed dispersal extends over a distance of only about 150 km. Though clast concentrations in this train are based on semiquantitative data, they seem distinctly lower than in the outlier I dispersal train. Lastly, the fact that the dispersal train from outlier II crosses the final position of the ice divide suggests that its formation was interrupted by the westward migration of the ice divide over a distance of about 150 km following the last glacial maximum.

Widespread evidence of basal sliding and abrasion recorded by striations associated with successive flow systems, together with the development of long dispersal trains, indicates that protracted warm-based conditions prevailed in north-central Quebec, the core region of the eastern Laurentide Ice Sheet. This conclusion is at variance with earlier interpretations of protracted cold-based conditions in core regions of the Laurentide Ice Sheet based on till lineation mapping from Landsat imagery and digital elevation models (Kleman et al., 1994; Kleman and Hättestrand, 1999; Kleman and Glasser, 2007), but it is in accord with thermomechanical modelling of the last glacial cycle (Marshall and Clark, 2002).

Kimberlite indicator minerals recovered from a survey of heavy minerals in eskers of the Saindon-Cambrien zone in north-central Quebec confirm the diamond exploration potential of the region. These results are in addition to G9 chrome-rich pyropes reported by Girard (1999) in a till survey east of our study area. Kimberlite indicator minerals were observed along two regional corridors intersecting at nearly right angles in the Lake Gayot (23-M) map area (Fig. 6). Although these corridors are parallel to prominent regional fracture sets, they also correspond to regional glacial dispersal directions. The regional dispersal models (Fig. 3, 5) suggest that the intersection zone in map area 23-M is a prime target for follow-up diamond exploration.

ACKNOWLEDGMENTS

First and foremost, I would like to dedicate this paper to my long-time friend and colleague Serge Paradis, with whom I shared several fieldwork seasons in northern Quebec, but who passed away too soon in early 2021. Financial support received under the Targeted Geoscience Initiative and the Northern Resources Development programs of Natural Resources Canada (Geological Survey of Canada) is gratefully acknowledged. I would like to thank Réjean Girard (IOS Services Géoscientifiques Inc.) for his key contribution in interpreting microprobe data. I would also like to thank colleagues at the Ministère des Ressources naturelles du Québec, Alain Leclair, Charles Gosselin, Alain Berclaz, Martin Parent, Martin Simard, Patrice Roy, and Jean-Yves Labbé, who generously shared their knowledge of northern Quebec geology and their basecamps over several field seasons. Harold Vigneault and Marco Boutin (INRS-Géoressources) prepared most of the figures. I also thank Éric Boisvert (Geological Survey of Canada) and Martin Ross (University of Waterloo) for their critical reviews of the first draft of this paper. Many thanks go to Isabelle McMartin (Geological Survey of Canada) for her scientific editing of this chapter.

REFERENCES

Allard, G., Roy, M., Ghaleb, B., Richard, P.J.H., Larouche, A.C., Veillette, J.J., and Parent, M., 2012. Constraining the age of the last interglacial–glacial transition in the Hudson Bay lowlands (Canada) using U–Th dating of buried wood; Quaternary Geochronology, v. 7, no. 1, p. 37–47. https://doi.org/10.1016/j.quageo.2011.09.004

Bamber, J.L., Vaughan, D.G., and Joughin, I., 2000. Widespread complex flow in the interior of the Antarctic Ice Sheet; Science, v. 287, no. 5456, p. 1248–1250. https://doi.org/10.1126/science.287.5456.1248

Baumgartner, M., Ankar, E., and Grütter, H., 2003. Compositional classification of 'kimberlitic' and 'non-kimberlitic' ilmenite, with implications for visual selection and discrimination; *in* International Kimberlite Conference, Victoria: Extended Abstracts, v. 8, 5 p. https://doi.org/10.29173/ikc3182

Beaumier, M., 2002. Données digitales d'un inventaire des minéraux lourds dans le till de la région d'Ashuanipi; données tirées des GM 59085 et 59086 de BHP; Ministère des Ressources naturelles du Québec, DP-2002-02, 1 .zip file. <https://gq.mines.gouv.qc.ca/documents/EXAMINE/DP200202/> [accessed December 4, 2022]

Bolduc, A.M., 1992. The formation of eskers based on their morphology, stratigraphy, and lithologic composition, Labrador, Canada; Ph.D. thesis, Lehigh University, Bethlehem, Pennsylvania, 190 p. <http://www.alwelaie.com/website/universitytheses_details_print.php?theses_id=20405> [accessed December 4, 2022]

Bouchard, M.A. and Martineau, G., 1985. Southeastward ice flow in central Quebec and its paleogeographic significance; Canadian Journal of Earth Sciences, v. 22, no. 10, p. 1536–1541. https://doi.org/10.1139/e85-159

C.F. Mineral Research Ltd., 1989. The development of advanced technology to distinguish between diamondiferous and barren diatremes; Geological Survey of Canada, Open File 2124, Parts I, II, and III, 1183 p. https://doi.org/10.4095/130799

Cummings, D.I. and Russell, H.A.J., 2018. Glacial dispersal trains in North America; Journal of Maps, v. 14, no. 2, p. 476–485. https://doi.org/10.1080/17445647.2018.1478752

Daigneault, R.A., 2008. Géologie du Quaternaire du nord de la péninsule d'Ungava, Québec; Geological Survey of Canada, Bulletin 533, 115 p. https://doi.org/10.4095/224807

Daigneault, R.A. and Bouchard, M.A., 2004. Les écoulements et le transport glaciaires dans la partie septentrionale du Nunavik (Québec); Canadian Journal of Earth Sciences, v. 41, no. 8, p. 919–938. https://doi.org/10.1139/e04-048

DiLabio, R.N.W. and Coker, W.B. (ed.), 1989. Drift prospecting; Geological Survey of Canada, Paper 89-20, 169 p. https://doi.org/10.4095/127357

Dimroth, E., 1978. Région de la Fosse du Labrador entre les latitudes 54°30′ et 56°30′ / Labrador Trough area between latitudes 54°30′ and 56°30′; Ministère des Richesses naturelles du Québec, Geological Report 193, 417 p.

Dressler, B. and Ciesielski, A., 1979. Région de la Fosse du Labrador (56°30′–57°15′); Ministère des Richesses naturelles du Québec, Geological Report 195, 136 p.

Dubé-Loubert, H., Roy, M., Veillette, J.J., Brouard, E., Schaefer, J.M., and Wittmann, H., 2021. The role of glacial dynamics in the development of ice divides and the Horseshoe intersection zone in the northeastern Labrador sector of the Laurentide Ice Sheet; Geomorphology, v. 387, art. no. 107777, 19 p. https://doi.org/10.1016/j.geomorph.2021.107777

Dyke, A.S. and Prest, V.K., 1987. Late Wisconsinan and Holocene history of the Laurentide Ice Sheet; Géographie physique et Quaternaire, v. 41, no. 2, p. 237–263. https://doi.org/10.7202/032681ar

Fipke, C.E., Gurney, J.J., and Moore, R.O., 1995. Diamond exploration techniques emphasising indicator mineral geochemistry and Canadian examples; Geological Survey of Canada, Bulletin 423, 86 p. https://doi.org/10.4095/205728

Gillberg, G., 1968. Lithological distribution and homogeneity of glaciofluvial material; Geologiska Föreningen i Stockholm Förhandlingar, v. 90, no. 2, p. 189–204. https://doi.org/10.1080/11035896809451882

Girard, R., 1999. Till mineralogy, Caniapiscau project, final report, BHP Minerals; Ministère des Ressources naturelles du Québec, GM 59086.

Gosselin, C. and Simard, M., 2000. Géologie de la région du lac Gayot (SNRC 23M); Ministère des Ressources naturelles du Québec, Geological Report 99-06, 29 p.

Gosselin, C., Simard, M., and David, J., 2001. Géologie de la région des lacs des Loups Marins (34A); Ministère des Ressources naturelles du Québec, Geological Report 2001-10, 37 p.

Gosselin, C., Roy, P., and David, J., 2002. Géologie de la région du lac Bienville (33P); Ministère des Ressources naturelles du Québec, Geological Report 2002-11, 38 p.

Gurney, J.J. and Moore, R.O., 1993. Geochemical correlations between kimberlitic indicator minerals and diamonds; *in* Diamonds: exploration, sampling and evaluation, short course; Prospectors and Developers Association of Canada, Toronto, p. 149–171.

Gurney, J.J. and Zweistra, P., 1995. The interpretation of the major element compositions of mantle minerals in diamond exploration; Journal of Geochemical Exploration, v. 53, no. 1-3, p. 293–309. https://doi.org/10.1016/0375-6742(94)00021-3

Hughes, O.L., 1964. Surficial geology, Nichicun–Kaniapiskau map-area, Quebec; Geological Survey of Canada, Bulletin 106, 20 p. https://doi.org/10.4095/100624

Klassen, R.A. and Thompson, F.J., 1993. Glacial history, drift composition, and mineral exploration, central Labrador; Geological Survey of Canada, Bulletin 435, 76 p. https://doi.org/10.4095/183906

Kleman, J. and Glasser, N.F., 2007. The subglacial thermal organisation (STO) of ice sheets; Quaternary Science Reviews, v. 26, no. 5-6, p. 585–597. https://doi.org/10.1016/j.quascirev.2006.12.010

Kleman, J. and Hättestrand, C., 1999. Frozen-bed Fennoscandian and Laurentide ice sheets during the last glacial maximum; Nature, v. 402, p. 63–66. https://doi.org/10.1038/47005

Kleman, J., Borgström, I., and Hättestrand, C., 1994. Evidence for a relict glacial landscape in Quebec–Labrador; Palaeogeography, Palaeoclimatology, Palaeoecology, v. 111, no. 3-4, p. 217–228. https://doi.org/10.1016/0031-0182(94)90064-7

Levasseur, D. and Prichonnet, G., 1995. La dispersion clastique des débris rocheux dans les eskers et le till adjacent de la région de Chapais–Chibougamau (Québec) au Wisconsinien supérieur; Canadian Journal of Earth Sciences, v. 32, no. 5, p. 590–602. https://doi.org/10.1139/e95-050

Lortie, G. and Martineau, G., 1987. Les systèmes de stries glaciaires dans les Appalaches du Québec; Ministère de l'Énergie et des Ressources du Québec, DV-85-10, 45 p.

Margold, M., Stokes, C.R., and Clark, C.D., 2018. Reconciling records of ice streaming and ice margin retreat to produce a palaeogeographic reconstruction of the deglaciation of the Laurentide Ice Sheet; Quaternary Science Reviews, v. 189, p. 1–30. https://doi.org/10.1016/j.quascirev.2018.03.013

Marshall, S.J. and Clark, P.U., 2002. Basal temperature evolution of North American ice sheets and implications for the 100-kyr cycle; Geophysical Research Letters, v. 29, no. 24, p. 67-1–67-4. https://doi.org/10.1029/2002GL015192

Melanson, A., Bell, T., and Tarasov, L., 2013. Numerical modelling of subglacial erosion and sediment transport and its application to the North American ice sheets over the last glacial cycle; Quaternary Science Reviews, v. 68, p. 154–174. https://doi.org/10.1016/j.quascirev.2013.02.017

Mitchell, R.H., 1986. Kimberlites: mineralogy, geochemistry, and petrology; Springer, New York, 442 p. https://doi.org/10.1007/978-1-4899-0568-0

Moorhead, J., Perrault, S., Berclaz, A., Sharma, K.N.M., Beaumier, M., and Cadieux, A.-M., 2000. Kimberlites et diamants dans le nord du Québec; Ministère des Ressources naturelles du Québec, PRO 2000-05, 9 p.

Moorhead, J., Beaumier, M., Girard, R., and Heaman, L., 2003. Distribution, structural controls and ages of kimberlite fields in the Superior Province of Quebec; *in* International Kimberlite Conference, Victoria: Extended Abstracts, v. 8, 5 p.

Nimis, P. and Taylor, W.R., 2000. Single clinopyroxene thermobarometry for garnet peridotite; part 1: calibration and testing of a Cr-in-Cpx barometer and an enstatite-in-Cpx thermometer; Contributions to Mineralogy and Petrology, v. 139, no. 5, p. 541–554. https://doi.org/10.1007/s004100000156

Parent, M. and Paradis, S.J., 1993. Interprétation préliminaire des écoulements glaciaires dans la région de la Petite rivière de la Baleine, région subarctique du Québec; *in* Current research, part C, Canadian Shield; Geological Survey of Canada, Paper 93-1C, p. 359–365. https://doi.org/10.4095/134263

Parent, M., Paradis, S.J., and Boisvert, É., 1995. Ice-flow patterns and glacial transport in the eastern Hudson Bay region: implications for the late Quaternary dynamics of the Laurentide Ice Sheet; Canadian Journal of Earth Sciences, v. 32, no. 12, p. 2057–2070. https://doi.org/10.1139/e95-159

Parent, M., Paradis, S.J., and Doiron, A., 1996. Palimpsest glacial dispersal trains and their significance for drift prospecting; Journal of Geochemical Exploration, v. 56, no. 2, p. 123–140. https://doi.org/10.1016/0375-6742(96)00011-8

Parent, M., Beaumier, M., and Paradis, S.J., 2002. A new high-potential target for diamond exploration in northern Quebec — chromium picroilmenites in esker sediments of the Lac Bienville (33P) region; Ministère des Ressources naturelles du Québec, PRO 2002-03, 4 p.

Parent, M., Paradis, S.J., and Beaumier, M. 2003. Dynamique glaciaire polyphasée et dispersion glacio-sédimentaire dans la région du lac Anuc (34 O), nord du Québec; *in* Projet de cartographie du Grand-Nord; Ministère des Ressources naturelles du Québec, Workshop Report MB 2003-01, p. 55–61.

Parent, M., Beaumier, M., Girard, R., and Paradis, S.J., 2004. Diamond exploration in the Archean craton of northern Québec — kimberlite indicator minerals in eskers of the Saindon-Cambrien corridor; Ministère des Ressources naturelles du Québec, MB 2004-02, 16 p.

Paulen, R.C. and McMartin, I., 2009. Application of till and stream sediment heavy mineral and geochemical methods to mineral exploration in western and northern Canada; Geological Association of Canada, Short Course Notes 18, 221 p.

Prest, V.K., 1984. The Late Wisconsinan glacier complex; *in* Quaternary stratigraphy of Canada — a Canadian contribution to IGCP Project 24, (ed.) R.J. Fulton; Geological Survey of Canada, Paper 84-10, p. 21–36. https://doi.org/10.4095/119756

Prest, V.K., Grant, D.R., and Rampton, V.N., 1968. Glacial map of Canada; Geological Survey of Canada, Map 1253A, scale 1:5 000 000. https://doi.org/10.4095/108979

Rice, J.M., Ross, M., Paulen, R.C., Kelley, S.E., Briner, J.P., Neudorf, C.M., and Lian, O.B., 2019. Refining the ice flow chronology and subglacial dynamics across the migrating Labrador Divide of the Laurentide Ice Sheet with age constraints on deglaciation; Journal of Quaternary Science, v. 34, no. 7, p. 519–535. https://doi.org/10.1002/jqs.3138

Rice, J.M., Ross, M., Paulen, R.C., Kelley, S.E., and Briner, J.P., 2020. A GIS-based multi-proxy analysis of the evolution of subglacial dynamics of the Quebec–Labrador ice dome, northeastern Quebec, Canada; Earth Surface Processes and Landforms, v. 45, no. 13, p. 3155–3177. https://doi.org/10.1002/esp.4957

Rignot, E., Mouginot, J., and Scheuchl, B., 2011. Ice flow of the Antarctic Ice Sheet; Science, v. 333, no. 6048, p. 1427–1430. https://doi.org/10.1126/science.1208336

Sharpe, D.R., Kjarsgaard, B.A., Knight, R.D., Russell, H.A.J., and Kerr, D.E., 2017. Glacial dispersal and flow history, East Arm area of Great Slave Lake, NWT, Canada; Quaternary Science Reviews, v. 165, p. 49–72. https://doi.org/10.1016/j.quascirev.2017.04.011

Shilts, W.W., 1980. Flow patterns in the central North American ice sheet; Nature, v. 286, p. 213–218. https://doi.org/10.1038/286213a0

Simard, M., Gosselin, C., and David, J., 2001. Géologie de la région du lac Maricourt (24D); Ministère des Ressources naturelles du Québec, Geology Report 2000-07, 50 p.

Sobolev, N.V., 1974. Deep-seated inclusions in kimberlites and the problem of the composition of the upper mantle; American Geophysical Union, Washington, D.C., 279 p. (translated by D.A. Brown).

USGS (United States Geological Survey), 2008. Shuttle Radar Topography Mission; mapping the world in 3 dimensions. <https://www2.jpl.nasa.gov/srtm/dataprelimdescriptions.html> [accessed November 24, 2022]

Veillette, J.J., 1986. Former southwesterly ice flows in the Abitibi–Timiskaming region: implications for the configuration of the late Wisconsinan ice sheet; Canadian Journal of Earth Sciences, v. 23, no. 11, p. 1724–1741. https://doi.org/10.1139/e86-159

Veillette, J.J., 1997. Le rôle d'un courant de glace tardif dans la déglaciation de la baie James; Géographie physique et Quaternaire, v. 51, no. 2, p. 141–161. https://doi.org/10.7202/033115ar

Veillette, J.J., Dyke, A.S., and Roy, M., 1999. Ice-flow evolution of the Labrador sector of the Laurentide Ice Sheet: a review, with new evidence from northern Quebec; Quaternary Science Reviews, v. 18, no. 8-9, p. 993–1019. https://doi.org/10.1016/S0277-3791(98)00076-6